

# *In situ* photoemission study of the room-temperature ferromagnet ZnGeP<sub>2</sub>:Mn

Y. Ishida<sup>1</sup>, D. D. Sarma<sup>2</sup>, K. Okazaki<sup>1</sup>, J. Okabayashi<sup>1</sup>, J. I. Hwang<sup>1</sup>,

H. Ott<sup>3</sup>, A. Fujimori<sup>1</sup>, G. A. Medvedkin<sup>4</sup>, T. Ishibashi<sup>4</sup>, K. Sato<sup>4</sup>

<sup>1</sup>*Department of Physics, University of Tokyo, Bunkyo-ku Tokyo 113-0033, Japan*

<sup>2</sup>*Solid State and Structural Chemistry Unit, Indian Institute of Science, Bangalore 560 012 India*

<sup>3</sup>*Institut für Experimentalphysik Freie Universität Berlin, Arnimallee 14 14195 Berlin, Germany and*

<sup>4</sup>*Tokyo University of Agriculture and Technology, Koganei Tokyo 184-8588, Japan*

(Dated: May 22, 2019)

The chemical states of the ZnGeP<sub>2</sub>:Mn interface, which shows ferromagnetism above room-temperature, has been studied by photoemission spectroscopy. Mn deposition on the ZnGeP<sub>2</sub> substrate heated to 400°C induced Mn substitution for Zn and then the formation of metallic Mn-Ge-P compounds. Depth profile studies have shown that Mn 3d electrons changed their character from itinerant to localized along the depth, and in the deep region, dilute divalent Mn species (< 5 % Mn) was observed with a coexisting metallic Fermi edge of non-Mn 3d character. The possibility of hole doping through Mn substitution for Ge and/or Zn vacancy is discussed.

PACS numbers: 79.60.Jv, 75.50.Pp, 75.70.Cn

The successful synthesis of the III-V-based ferromagnetic diluted magnetic semiconductors (DMSs) has opened up a large number of exciting functionalities such as non-volatile memories, spin injection, and the optical control of ferromagnetism in semiconductor devices [1]. However, the reported Curie temperature ( $T_C$ ) to date has been limited to 120 K realized in Ga<sub>1-x</sub>Mn<sub>x</sub>As, due to the limited ability of incorporating Mn ions and *p*-type carriers in the III-V-based DMS. Overcoming this limitation and increasing the  $T_C$  hopefully above the room temperature (RT) has been a challenging subject.

Recently, there have been several reports on high- $T_C$  ferromagnetism in new DMSs [2]. Among them are intriguing reports by Medvedkin *et al.* on Mn incorporated II-IV-V<sub>2</sub> chalcopyrite semiconductors CdGeP<sub>2</sub> [3] and ZnGeP<sub>2</sub> [4], which show ferromagnetism above RT. A high concentration of Mn ions is incorporated in the semiconductors through deposition of Mn metal and annealing. The use of II-IV-V<sub>2</sub> semiconductor as a host material is attracting, since, while it is an average III-V semiconductor, it has two types of cation sites. This distinct property compared to the binary III-V semiconductors allows us to functionalize each cation site in different ways, e.g., magnetic ion doping at the II site and acceptor doping at the IV site. In addition, the chalcopyrite semiconductors have many natural defects, e.g., zinc ion on the germanium site (Zn<sub>Ge</sub>), zinc vacancy (V<sub>Zn</sub>), etc, in ZnGeP<sub>2</sub>, which may also act as acceptors [5]. This rich chemistry stimulated many theoretical calculations on II-IV-V<sub>2</sub>:Mn [6]. However, there has been little experimental information about the chemical reactions and chemical products in this system.

Photoemission spectroscopy (PES) is a powerful tool to investigate chemical reactions in surface and interfacial regions. Particularly for studying the Mn-doped chalcopyrites, where the Mn density varies as a function of the depth, PES combined with ion sputtering provides us with the depth profile of the interface. At the same time, PES provides insight into the electronic structures

of DMSs [7], particularly into the Mn 3d partial density of states (PDOS) through resonant PES and through subsequent analyses of the *p-d* exchange interaction between the Mn 3d electrons and the host semiconductors.

Ultraviolet photoemission (UPS) and x-ray photoemission (XPS) measurements were performed at BL-18A of Photon Factory. The total energy resolution of the VG CLAM analyzer including temperature broadening was 800 meV for XPS and 200 meV for UPS. Mn metal (99.999 %) was evaporated *in situ* onto the (001) surface of single crystal ZnGeP<sub>2</sub> at 400°C [4]. The deposition rate was 3 Å/min, determined by a quartz thickness monitor. After the Mn deposition, the sample was post-annealed at 400°C for 5 min and then cooled to RT. All the spectra were taken at RT. Ar<sup>+</sup>-ion sputtering at 1.5 kV was used both for cleaning and etching. Sputter-etching rate was ~ 2 Å/min. Surface cleanliness was checked by core-level XPS. The pressure was below  $7 \times 10^{-10}$  Torr during the measurements. The magnetization was measured *ex situ* using a SQUID magnetometer. (Quantum Design MPMS). For comparison, polycrystalline MnP ( $T_C = 290$  K [8]) was also measured.

First, the effect of annealing and sputtering on the ZnGeP<sub>2</sub> substrate was studied. The core-level intensities above 300°C showed strong Zn deficiency and weak Ge excess. [See the relative chemical composition at  $d = 0$  Å in Fig. 1(b), where the deviation from the stoichiometry of ZnGeP<sub>2</sub> is seen for the surface once annealed at 400°C.] At the reported “optimum” substrate temperature 400°C, therefore, deposited Mn atoms may easily diffuse into the Zn-deficient surface region. This Zn-deficient region could be removed by 3-min Ar<sup>+</sup>-ion sputtering (corresponding to ~ 6 Å thickness). Further sputtering did not change the core-level intensities of the substrate within the accuracy of 3 %. This suggests that selective sputtering of different atomic species can be ignored, and we assumed that the as-sputtered substrate spectra represent the bulk stoichiometry of ZnGeP<sub>2</sub>.

Next we show a series of spectra for Mn deposition

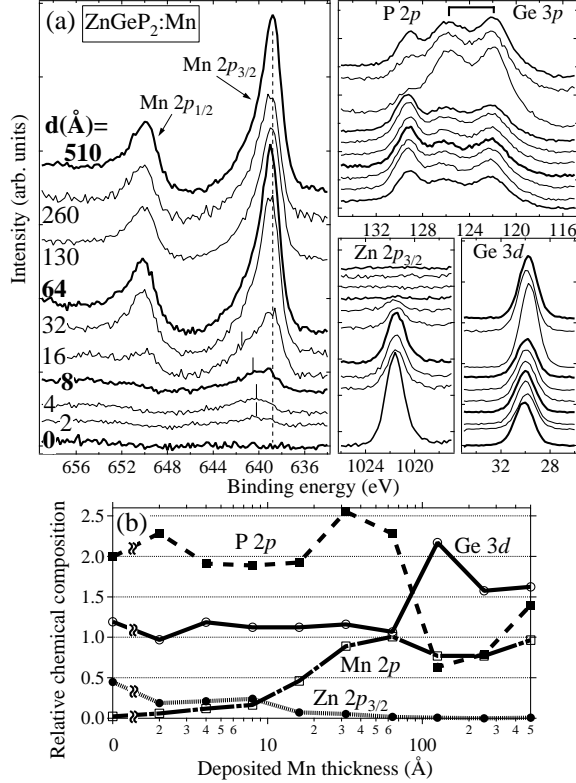


FIG. 1: Core-level spectra of  $\text{ZnGeP}_2\text{:Mn}$  for various Mn thickness deposited at  $400^\circ\text{C}$ . (a) Raw spectra. The vertical scale is counts per second. 0 Å corresponds to the sputtered and annealed surface of the  $\text{ZnGeP}_2$  substrate. (b) Core-level intensities as functions of deposited Mn thickness. For normalization, see text.

on the  $400^\circ\text{C}$ -annealed substrate. Each time after having taken a set of spectra for one Mn coverage, the deposited Mn was completely removed by prolonged sputtering and then Mn was newly deposited. Figure 1(a) shows the core-level spectra of the Mn-deposited surface, and Fig. 1(b) shows their intensities normalized to those for the as-sputtered  $\text{ZnGeP}_2$ . The Mn  $2p$  intensity has been normalized using the Mn  $2p$  and P  $2p$  intensity ratio of MnP. In the region of Mn thickness  $d < 64$  Å, one can see a monotonic increase and decrease of the Mn and Zn signals, respectively, without significant changes in the Ge and P intensities. This behaviour suggests that Mn atoms primarily substituted for Zn and a  $\text{Zn}_{1-x}\text{Mn}_x\text{GeP}_2$ -like compound was formed. In the Mn  $2p_{3/2}$  spectra below  $d = 16$  Å, one can see some signal on the higher binding energy side [indicated by vertical bars in Fig. 1(a)] of the dominant metallic peak ( $E_B = 638.7$  eV, broken line). This indicates that a portion of the incorporated Mn atoms chemically reacted with the substrate and presumably became  $\text{Mn}^{2+}$ . In going from  $d = 64$  to  $130$  Å, the Ge and P intensities suddenly changed. The saturation of the Mn intensity with sizable signals

of Ge and P above  $d = 130$  Å is a signature of atomic diffusion associated with the chemical reaction for such a thick Mn overlayer. The surface region above  $d = 130$  Å consisted of Ge-rich, ternary metallic compound(s) of Mn, Ge, and P with possible inhomogeneity and/or phase mixture.

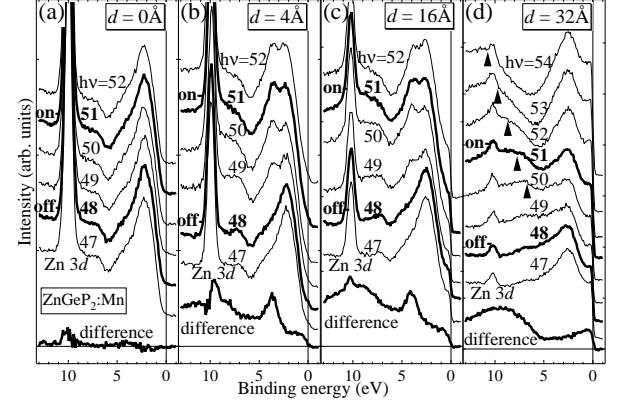


FIG. 2: Valence-band spectra of  $\text{ZnGeP}_2\text{:Mn}$  in the  $3p$ - $3d$  core excitation region. On- and off-resonance energies are 51 eV and 48 eV, respectively, and the spectra at the bottom show their difference spectra. Triangles in (d) indicate the constant kinetic energy of the Mn  $M_3L_{4,5}L_{4,5}$  Auger signal.

The valence-band spectra taken for photon energies in the Mn  $3p$ - $3d$  core-excitation region are shown in Fig. 2. The spectra have been primarily normalized to the post-focusing Au mirror current and then to the intensities of the  $d = 0$  Å spectra at the corresponding photon energies. The Mn  $3d$ -driven spectra were obtained by subtraction between these normalized on- (51 eV) and off-resonance (48 eV) spectra. In this way, we could virtually eliminate the effect of the photon energy dependence of the host valence band. For  $d = 4$  and  $16$  Å, one can see a peak located  $\sim 4$  eV below  $E_F$  in the difference spectra. This observation is similar to the previous results of the Mn incorporated II-VI- and III-V-based DMSs [7] and thus is attributed to the localized nature of Mn  $3d$  electrons. However, above  $d = 32$  Å, there was a change in the decay process of the Mn  $3p$  core hole and strong Mn  $M_3L_{4,5}L_{4,5}$  Auger peak replaces the  $\sim 4$  eV peak, indicating that the Mn  $3d$  electrons became itinerant. The disappearance of the  $\sim 4$  eV peak is in accordance with the Mn  $2p$  core-level spectrum [Fig. 1(a)], where the divalent Mn signal disappeared above  $d = 32$  Å and the highly asymmetric line shape characteristic of a metallic Mn compound appeared. We note that MnP also shows Mn  $M_3L_{4,5}L_{4,5}$  Auger signals in the valence-band spectra [9]. However, the Mn  $2p_{3/2}$  core-level peak of MnP was observed at  $E_B = 639.2$  eV, different from the peak positions observed above  $d = 32$  Å in Fig. 1(a). As for the  $d = 16$  Å spectrum, both a clear Fermi edge and the  $\sim 4$  eV peak is observed. The difference spectrum for  $d = 16$  Å is almost a superposition of the  $d = 4$  and  $32$

Å spectra, as in the case of the Mn 2*p* core-level spectra [Fig. 1(a)].

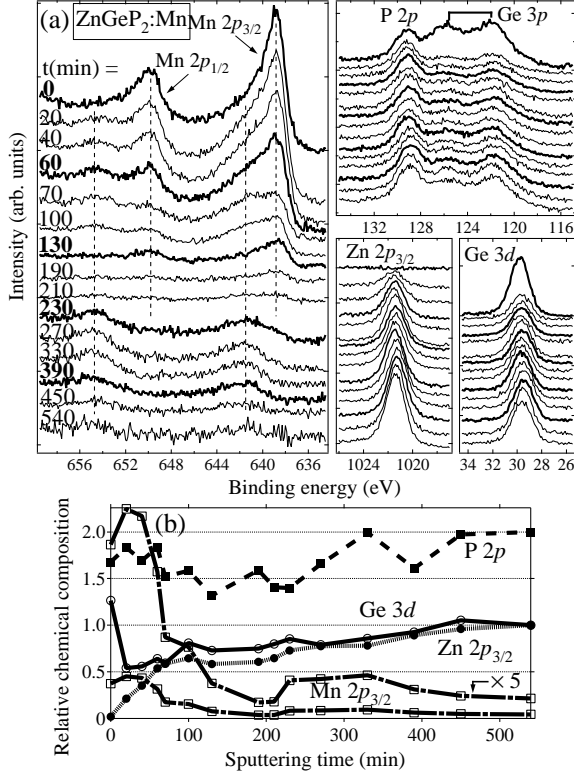


FIG. 3: Core-level spectra of ZnGeP<sub>2</sub>:Mn in the depth profile. (a) Raw spectra. The vertical scale is counts per second. (b) Core-level intensities as functions to sputtering time.

In order to study the chemical states formed underneath the surface metallic compound(s), ZnGeP<sub>2</sub>:Mn of the nominal Mn thickness of 150 Å was repeatedly sputter-etched without annealing and studied by PES. Figure 3 (a) shows core-level spectra taken in the sputter-etching series and Fig. 3 (b) shows their intensities [the same normalization as in Fig. 1 (b)] as functions of sputtering time. The change in the first 20 min sputtering is attributed to the removal of the metallic Mn-Ge-P layer in the surface region. Subsequently, the Mn 2*p*<sub>3/2</sub> core level started to show a shoulder structure at  $E_B = 641.7$  eV due to ionic Mn (Mn<sup>2+</sup> most likely). The systematic increase of this shoulder and the decrease of the metallic main peak between 20 to 70 min sputtering indicate that these signals are originated from chemically different Mn species. After 100 min sputtering, the relative compositions became Zn:Ge:P ~ 1:1:2, suggesting that the chalcopyrite-type matrix of Zn, Ge, and P plus dilute Mn was exposed [Fig. 3 (b)]. After 230 min sputtering, the Mn signal became totally that of the ionic one [Fig. 3 (a)], indicating that a dilute-Mn phase (< 5 % Mn) appeared. Since Zn:Ge:P ~ 1:1:2 and the amount of Mn was small, it was difficult to determine from Fig. 3(b)

which element Mn substituted for. Now, since the peak position of the ionic Mn 2*p* signal below ~ 200 min sputtering (in the intermediate phase) corresponds to that above ~ 200 min sputtering (dilute Mn phase), the ionic Mn species in the former phase region may be precursors of those in the latter phase.

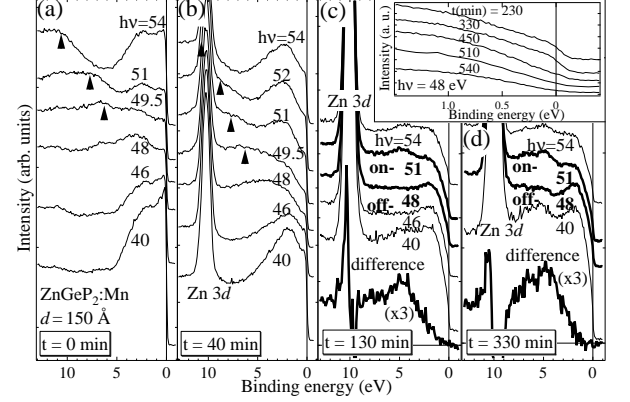


FIG. 4: Valence-band spectra of ZnGeP<sub>2</sub>:Mn ( $d = 150$  Å) in the sputter-etching series. Triangles in (a) and (b) denote the  $M_3L_{4,5}L_{4,5}$  Auger signals. Inset shows the valence-band spectra near  $E_F$  for sputtering time longer than 230 min.

Figure 4 shows the valence-band spectra in the sputter-etching series for photon energies in the Mn 3*p*-3*d* core excitation region. Before 80 min sputtering, the  $M_3L_{4,5}L_{4,5}$  Auger process was dominant [Fig. 4 (a) and (b)] and after that resonant photoemission became dominant [Fig. 4 (c) and (d)]. This indicates again that the Mn 3*d* states changed their character from itinerant to localized along the depth profile. A peak at  $E_B \sim 4$  eV was seen after 80 min sputtering, and hence Mn was divalent in the deep region. The divalent Mn signal in the recent EPR measurements may come from this region [10]. The Mn 3*d*-derived intensity near  $E_F$  in the difference spectra is weak compared to that in Fig. 2 (b). This indicates that the Mn 3*d* states are more strongly localized in the deep bulk region than the Zn<sub>1-x</sub>Mn<sub>x</sub>GeP<sub>2</sub>-like phase in the early stage of Mn deposition. Inset of Fig. 4 shows valence-band spectra near  $E_F$  after 230 min sputtering, where Mn had fully reacted with the substrate [Fig. 3 (a)]. They clearly show a Fermi edge. Since the Mn 3*d* PDOS is suppressed near  $E_F$ , this Fermi edge comes from the valence band of the host semiconductor which was somehow doped with metallic charge carriers. Since isovalent substitution of Mn<sup>2+</sup> for Zn<sup>2+</sup> cannot produce carriers, Mn<sup>2+</sup> may have substituted for the Ge site and/or Mn incorporation simultaneously induced defects such as, e.g.,  $V_{Zn}$  and  $Zn_{Ge}$ , all of which produce hole carriers. The Fermi edge became obscure after 540 min sputtering, in accordance with the diminishing Mn 2*p* core-level intensity (Fig. 3). In the sputter-etching series, too, no MnP signal was observed.

We have also studied the depth profile of ZnGeP<sub>2</sub>:Mn of the 200 Å nominal thickness Mn annealed at 200°C. Up

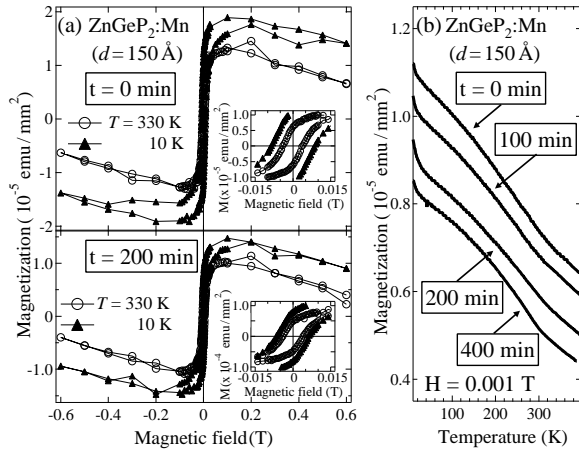


FIG. 5: Magnetization per sample area of  $\text{ZnGeP}_2\text{:Mn}$  ( $d = 150 \text{ \AA}$ ) prepared at  $400^\circ\text{C}$ . (a) Magnetization curves at  $T = 10 \text{ K}$  and  $330 \text{ K}$  of as-prepared  $\text{ZnGeP}_2\text{:Mn}$  (upper) and those after having removed the surface metallic Mn compound (lower). From these data, magnetization per Mn atom is crudely estimated to be  $1.5 \mu_B$ . Insets show the magnified plot revealing hysteresis. (b) Magnetization versus temperature in the sputtering series.

to 800 min sputtering, Mn signal was observed together with Zn, Ge, and P signals, indicating that diffusive reaction of Mn into the substrate occurred already at  $200^\circ\text{C}$ . However, the Mn  $2p_{3/2}$  signal always appeared at  $E_B = 638.7 \text{ eV}$  without any divalent signal. Correspondingly, only the Mn  $M_3L_{4,5}L_{4,5}$  Auger peak was observed in the valence-band spectra. We therefore conclude that the annealing at  $200^\circ\text{C}$  was insufficient for the Mn atoms to be chemically incorporated in the host semiconductor as divalent ions with localized nature of Mn  $3d$  electrons.

Figure 5(a) shows the magnetization of as-prepared  $\text{ZnGeP}_2\text{:Mn}$  ( $d = 150 \text{ \AA}$  at  $400^\circ\text{C}$ ) and that after having removed the surface metallic Mn compound (200 min sputtered). Clear hysteresis was observed between 10 K and 330 K for the 150 Å deposited sample. Surprisingly, one can observe nearly the same magnetization at both 330 K and 10 K even after removing the surface metal-

lic Mn compound, indicating that the divalent Mn phase deep in the substrate ( $< 5 \%$  Mn) was probably a RT ferromagnet. Figure 5(b) clearly shows ferromagnetism up to  $\sim 400 \text{ K}$ . One can see a kink at  $\sim 300 \text{ K}$  which may correspond to the  $T_C = 312 \text{ K}$  of bulk  $\text{Zn}_{1-x}\text{Mn}_x\text{GeP}_2$  [11]. Another anomaly at 20 - 50 K may also correspond to the 47 K anomaly of bulk  $\text{Zn}_{1-x}\text{Mn}_x\text{GeP}_2$ . Therefore, the present sample may contain  $\text{Zn}_{1-x}\text{Mn}_x\text{GeP}_2$  as a minority component. Recently,  $\text{ZnGeP}_2\text{:Mn}$  prepared at  $550^\circ\text{C}$  was studied, and the  $M(T)$  curve showed pronounced singularities at  $\sim 318 \text{ K}$  and 20 - 50 K and small magnetization tailing above 318 K, the behaviour of which is more similar to bulk  $\text{Zn}_{1-x}\text{Mn}_x\text{GeP}_2$  than the present sample [12]. We note that the bulk  $\text{Zn}_{1-x}\text{Mn}_x\text{GeP}_2$  was reported to be electrically insulating, while the present sample showed a metallic Fermi edge. Further studies are necessary, in particular to understand the relationship between the magnetic behaviour, the carrier density, and the preparation temperature.

In conclusion, we have observed spectral features of localized, most likely divalent Mn  $3d$  states incorporated into the host  $\text{ZnGeP}_2$  in the thin Mn-deposited surface region (probably as a  $\text{Zn}_{1-x}\text{Mn}_x\text{GeP}_2$ ) and in deep region below the surface metallic Mn compound after thick Mn deposition. A Fermi edge was observed in the deep region, indicating that carrier doping took place in that region of  $\text{ZnGeP}_2\text{:Mn}$ . RT ferromagnetism was observed after removing the surface Mn compound. This indicates that ferromagnetism in  $\text{ZnGeP}_2\text{:Mn}$  is caused by the dilute Mn ions in the deep region. No signature of MnP was observed in the photoemission spectra.

We thank T. Okuda, A. Harasawa, and T. Kinoshita for their valuable technical help, V.G. Voevodin, K. Ono, T. Komatsubara, and M. Okusawa for sample measurements, and T. Mizokawa for useful discussions and suggestions. This work was supported by a Grant-in-Aid for Scientific Research in Priority Area "Semiconductor Spintronics" (No. 14076209) from the Ministry of Education, Culture, Sports, Science and Technology, Japan. DDS thanks the University of Tokyo for hospitality during a part of this work. The experiment at Photon Factory was approved by the Photon Factory Program Advisory Committee (Proposal No. 01U005).

- [1] H. Ohno, F. Matsukura, and Y. Ohno, JSAP International No.5, 4 (2002), and references therein.
- [2] K. Ueda, H. Tabata, and T. Kawai, Appl. Phys. Lett. **79**, (2001) 988; H. Saeki, H. Tabata, and T. Kawai, Solid State Commun. **120**, (2001) 439; Y. Matsumoto *et al.*, Jpn. J. Appl. Phys. **40**, (2001) L1204; S. Kuwabara *et al.*, Jpn. J. Appl. Phys. **40**, L724 (2001); S. Sonoda *et al.*, J. Cryst. Growth **237-239** 1358 (2002).
- [3] G.A. Medvedkin *et al.*, Jpn. J. Appl. Phys. **39** L949 (2000); K. Sato *et al.*, J. Appl. Phys. **88**, 7027 (2001).
- [4] G.A. Medvedkin *et al.*, J. Cryst. Growth **236**, 609 (2002); K. Sato, G.A. Medvedkin, and T. Ishibashi, J. Cryst.

- Growth **237 - 239**, 1363 (2002).
- [5] S.D. Setzler *et al.*, J. Appl. Phys. **86**, 6677 (1999); W. Gehlhoff *et al.*, Physica B **308-310**, 1015 (2001).
- [6] P. Mahadevan and A. Zunger, Phys. Rev. Lett. **88**, 047205 (2002); Y.-J. Zhao *et al.*, Phys. Rev. B **63**, 201202 (2001); Y.-J. Zhao *et al.*, Phys. Rev. B **65**, 094415 (2002); T. Kamatani and H. Akai, Phase Transition, in press.
- [7] L. Ley *et al.*, Phys. Rev. B **35**, 2839 (1987); J. Okabayashi *et al.*, Phys. Rev. B **59**, R2486 (1999); T. Mizokawa *et al.*, Phys. Rev. B **65** 085209 (2002); J. Okabayashi *et al.*, Phys. Rev. B **65** R161203 (2002).
- [8] E.E. Huber Jr. and D.H. Ridgley, Phys. Rev. **135** A 1033

- (1964).
- [9] A. Kakizaki *et al.*, J. Phys. Soc. Jap. **49**, 2183 (1980).
  - [10] P.G. Baranov *et al.*, J. Supercond., in press.
  - [11] S. Cho *et al.*, Phys. Rev. Lett. **88**, 257203 (2002).
  - [12] G.A. Medvedkin, P.G. Baranov, and S.I. Goloshchapov, J. Phys. Chem. Solids, in press.